Article ID: 1000-324X(2021)06-0652-07　　**DOI:** 10.15541/jim20200508

Directionally Solidified $Al_2O_3/Er_3Al_5O_{12}$ and $Al_2O_3/Yb_3Al_5O_{12}$ Eutectic Ceramics Prepared by Optical Floating Zone Melting

SUN Luchao[1], ZHOU Cui[1,2], DU Tiefeng[1], WU Zhen[1], LEI Yiming[1,2], LI Jialin[1], SU Haijun[3], WANG Jingyang[1]

(1. Shenyang National Laboratory for Materials Science, Institute of Metal Research, Chinese Academy of Sciences, Shenyang 110016, China; 2. School of Materials Science and Engineering, University of Science and Technology of China, Shenyang 110016, China; 3. State Key Laboratory of Solidification Processing, Northwestern Polytechnical University, Xi'an 710072, China)

Abstract: $Al_2O_3/Er_3Al_5O_{12}$(ErAG) and $Al_2O_3/Yb_3Al_5O_{12}$(YbAG) eutectic rods with fine and homogeneous microstructure, free from cracks or pores, were directionally solidified using optical floating zone method at growth rate of 10 mm/h. The crystallographic orientation, preferred orientation, and 3D distribution of Al_2O_3 and $Er_3Al_5O_{12}/Yb_3Al_5O_{12}$ phases in the terminal growth zone of Al_2O_3/ErAG and Al_2O_3/YbAG eutectics were investigated by EBSD and high-resolution X-ray microscope. Vickers hardness of the as-prepared Al_2O_3/ErAG and Al_2O_3/YbAG eutectics are determined as (13.5±0.4) and (12.8±0.1) GPa, respectively. The fracture toughness results of Al_2O_3/ErAG and Al_2O_3/YbAG are (3.0±0.2) and (3.2±0.1) MPa·$m^{1/2}$, respectively.

Key words: directional solidification; eutectic ceramic; microstructure; mechanical property

Directionally solidified eutectic oxide composites have been attracting extensive attentions as materials for very high temperature structural applications because of their unique properties, such as high melting point, excellent thermal and chemical stability in oxidizing atmospheres, microstructural stability up to temperatures very close to the melting point, and superior high-temperature strength retention and creep resistance[1-3]. Among them, Al_2O_3-based binary and ternary eutectics in Al_2O_3-ZrO_2-Y_2O_3 system are the most widely studied materials in the past years. It is reported that the binary $Al_2O_3/Y_3Al_5O_{12}$(YAG) eutectic composite fabricated by Bridgman method shows extremely stable microstructures, which remains un-growth after heat-treatment at 1973 K for 1000 h in air[1]. For binary Al_2O_3/YAG eutectic composite, a flexural strength of 2 GPa at ambient temperature was reported by Pastor, *et al*. and this strength could remain practically constant up to 1700 K[4]. The highest flexure strength of ternary Al_2O_3-YAG-ZrO_2 eutectic, determined by three-point bend testing, was (4.6±0.1) GPa, which was approximately four times higher than the best results measured in bulk non-oxide ceramics, such as SiC and Si_3N_4[5]. For the fracture toughness, a value as high as 8 MPa·$m^{1/2}$, has been reported for the laser melt-grown ternary Al_2O_3-YAG-ZrO_2 eutectic by Zhang, *et al*.[6]. All these studies demonstrated the outstanding mechanical properties of directionally solidified eutectic ceramics.

More recently, research hotspots have spread to the development of new oxide binary compounds, such as $Al_2O_3/RE_3Al_5O_{12}$ (RE=Er and Yb), to further improve the mechanical properties or to expand the potential application fields of directionally solidified eutectic oxide composites. Nakagawa and Waku, *et al*.[7] developed unidirectionally solidified $Al_2O_3/Er_3Al_5O_{12}$ (ErAG) binary eutectic and found that the composite possessed excellent thermally stability while strength at room temperature could be maintained up to 2073 K. Martinez, *et al*.[8] reported that Al_2O_3/ErAG binary system exhibited excellent creep resistance property up to 1550 ℃, which was 3 or 4 orders of magnitude better than 15° off *c*-axis sapphire. Mesa, *et al*.[9-10] successfully prepared Al_2O_3/ErAG eutectic rods by directional solidification, using the laser-heated floating zone method. The bend strength of these rods reached the maximum value of 2.7 GPa, which could be remained constant up to temperature about 1300 K. Besides the above excellent

Received date: 2020-09-01; **Revised date:** 2020-09-29; **Published online:** 2020-10-23
Foundation item: The State Key Laboratory of Solidification Processing (Northwestern Polytechnical University) (SKLSP201909); National Science and Technology Major Project (2017-VI-0020-0093); National Natural Science Foundation of China (51772302); International Cooperation Key Program(174321KYSB20180008)
Biography: SUN Luchao(1984–), male, associate professor. E-mail: lcsun@imr.ac.cn
孙鲁超(1984–), 男, 副研究员. E-mail: lcsun@imr.ac.cn
Corresponding author: WANG Jingyang, professor. E-mail: jywang@imr.ac.cn; SU Haijun, professor. E-mail: shjnpu@nwpu.edu.cn
王京阳, 研究员. E-mail: jywang@imr.ac.cn; 苏海军, 教授. E-mail: shjnpu@nwpu.edu.cn

thermal stability and mechanical properties at high temperatures, it is also believed that rare earth ions in the crystals may emit radiation in narrow bands. These comprehensive properties make directionally solidified eutectics promising candidates that can meet the thermo-structural challenges in thermofotovoltaic (TPV) converter applications[11-16]. The selective thermal emission results illustrated that Al_2O_3/ErAG showed intense emission band and could match with the GaSb photovoltaic cells[17] and $Al_2O_3/Yb_3Al_5O_{12}$(YbAG) showed an intense selective emission band at 1 μm, which was compatible with the silicon photovoltaic cells[18-19].

All of the above-mentioned researches have clearly illustrated directionally solidified Al_2O_3/ErAG and Al_2O_3/YbAG eutectics as promising materials for both high temperature structural and functional applications. However, studies on directionally solidified Al_2O_3/REAG eutectic ceramics, especially for Al_2O_3/YbAG eutectic, are still limited. Further studies on the solidification parameters optimization, microstructures evolution control and thermo-mechanical properties tailoring are still necessary. In this work, directionally solidified Al_2O_3/ErAG and Al_2O_3/YbAG eutectic composites were prepared using the optical floating zone melting method. This method can provide a stable and big melting zone at the liquid/solid interface, which is the key point for the growth of crack-free and low stress eutectic samples and is beneficial to attain eutectic rods with uniform and homogeneous microstructures. The composition and microstructure characteristics (phase distributions, selected orientations, and interfacial relationships) of the as-received eutectics were investigated specifically. The mechanical properties, including Vickers hardness and fracture toughness were evaluated and discussed combined with the microstructures.

1　Experimental procedure

Commercially available powders RE_2O_3 (RE= Er and Yb) (Rare-Chem. Hi-Tech. Co., Ltd., Huizhou, China) and Al_2O_3 (Sinopharm Chemical Reagent Co., Ltd., Shanghai, China) were used to fabricate the Al_2O_3/ErAG and Al_2O_3/YbAG eutectic composites. The powders were mixed according to the binary eutectic compositions with $n(Al_2O_3):n(Er_2O_3)=81:19$[20] and $n(Al_2O_3):n(Yb_2O_3)=81.5:19.5$[21], respectively. The starting powders were ball milled for 24 h in a Si_3N_4 jar, with Si_3N_4 balls and ethanol as media. The obtained slurry was dried at 60 ℃ for 24 h and then passed through a 75 μm (200-mesh) sieve, and then synthesized at 1550 ℃ for 6 h. The as-received powders were then cold pressed under a pressure of about 30 MPa for 15 min in a die steel mold, followed by cold isostatic pressing at 280 MPa for 15 min. The cold pressed bars were then sintered at 1550 ℃ for 2 h. The directional solidification experiments were conducted by an optical floating zone furnace equipped with four 3 kW xenon arc lamps as heat sources. The directional solidification process was conducted in argon atmosphere with a polycrystalline alumina rod as seed crystal. The directional solidification growth speed was set at 10 mm/h.

Phase composition of the as prepared directionally solidified eutectics was determined using X-ray diffractometer (D/max-2400, Rigaku, Tokyo, Japan). Microstructures of the longitudinal sections were observed with a scanning electron microscope (Supra 35, Zeiss, Oberkochen, Germany) equipped with an electron- dispersive spectrometer (EDS) and backscatter electron detector (BSED). The average eutectic spacing was estimated according to the arithmetic mean value of about 200–400 eutectic lamellar spacings which were crossed by 15 straight lines in the SEM images. The reconstructed 3D microstructures were investigated *via* a high-resolution X-ray microscope (Xradia Versa XRM-500, Zeiss, Oberkochen, Germany). The Vickers hardness (H_V) and the indentation fracture toughness (K_{IC}) were measured on polished longitudinal cross-sections, using a microhardness tester (432SVD, Wolrert, Shanghai, China), under loads (P) of 3, 5, 10, 30, and 50 N with a dwell time of 15 s. Five indentations were performed for each load and the hardness was quantified taking the average lengths of the indentation diagonals (d) using the following equation:

$$H_V=1.8544\frac{P}{d^2} \tag{1}$$

The indentation fracture toughness (K_{IC}) was calculated based on Anstis' model in Eq. (2), where c is the length of cracks emerging from indentation corners and E is the composite Young's modulus[22]:

$$K_{IC}=0.016\left(\frac{E}{H_V}\right)^{1/2}\left(\frac{P}{c^{3/2}}\right) \tag{2}$$

2　Results and discussion

Fig.1 shows the optical micrographs of the as received directionally solidified Al_2O_3/ErAG and Al_2O_3/YbAG eutectics. The as-grown eutectic rods are both with an average diameter in about 11 mm and length in about 90 mm, of which Al_2O_3/ErAG eutectic rod is pink and Al_2O_3/YbAG eutectic is blue. The surfaces of the rods are dense and smooth without any obvious pores while some slight skin-core structures could be observed in the transverse cross sections of both the eutectics. Samples

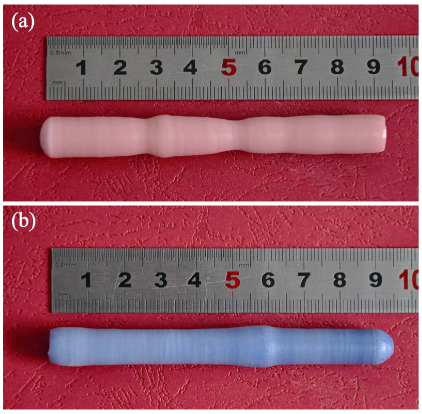

Fig. 1 Optical micrographs of the directionally solidified eutectics
(a) Al_2O_3/ErAG; (b) Al_2O_3/YbAG

cut from the end of these rods with a growth distance about 80–90 mm were chosen for the following phase composition, microstructure, and mechanical properties characterization.

The XRD patterns of the as-prepared directionally solidified Al_2O_3/ErAG and Al_2O_3/YbAG eutectics are shown in Fig. 2(a, b), respectively. It can be seen that both eutectics contain two phases: Al_2O_3 and $RE_3Al_5O_{12}$ phases, without diffraction peaks of other phases detected, which means the as-prepared eutectics are composed of Al_2O_3 and $RE_3Al_5O_{12}$.

The SEM morphologies of the transverse section of directionally solidified eutectics are exhibited in Fig. 3(a, b), respectively. A homogeneous and voids-free microstructure could be observed with only two phases in each sample. The light aeras are the ErAG and YbAG phases and the dark aeras are the Al_2O_3 phase in Fig. 3. The three-dimensional interpenetrating network of Al_2O_3 and REAG phases, which is a typical microstructure characteristic in directionally solidified eutectics and commonly referred to as “Chinese Script” microstructure, could be identified in both samples. It should be noticed that the size of the eutectic phases in these two eutectics are distinctly different. The average interlamellar spacing of as-prepared Al_2O_3/ErAG and Al_2O_3/YbAG eutectics are measured to be 6.9 and 17.2 μm, respectively.

The crystallographic relationships of Al_2O_3 and REAG phases of the as-grown eutectics were investigated by electron backscattering diffraction (EBSD) method. Also, we chose the end parts of the rods with a growth distance of 80–90 mm for EBSD observation. Fig. 4 show the EBSD maps and corresponding inverse pole figures (inserts) of Al_2O_3/ErAG (a,b) and Al_2O_3/YbAG (c,d). For Al_2O_3/ErAG, it is seen that the preferred growth directions of Al_2O_3 is $<10\bar{1}0>$. What should be mentioned is that there are two different colors in Fig. 4(a), which reveal two twin-related variants of Al_2O_3 and correspond to the same $<10\bar{1}0>$ orientation, since the $[10\bar{1}0]$ and $[0\bar{1}10]$ directions are not strictly equivalent and cannot be identified by electron diffraction for Al_2O_3.

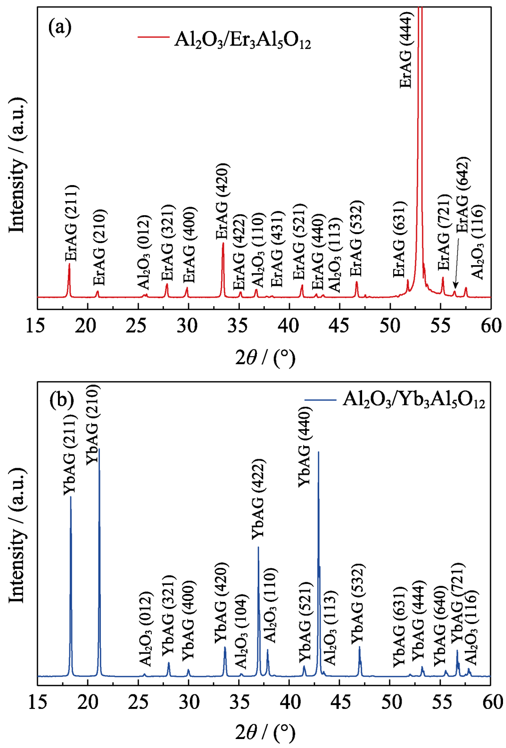

Fig. 2 XRD patterns of the directionally solidified eutectics
(a) Al_2O_3/ErAG; (b) Al_2O_3/YbAG

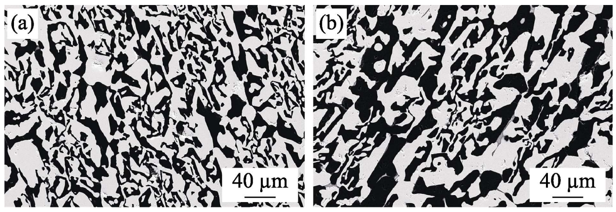

Fig. 3 SEM morphologies of the transverse section of directionally solidified eutectics
(a) Al_2O_3/ErAG; (b) Al_2O_3/YbAG

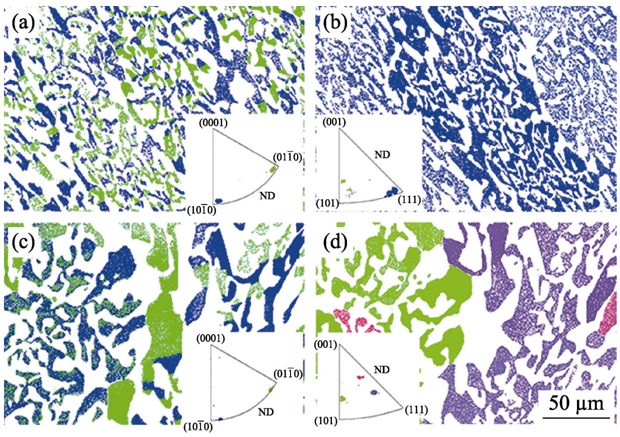

Fig. 4 EBSD maps and corresponding inverse pole figures (inserts) of Al_2O_3/ErAG ((a) Al_2O_3 and (b) ErAG) and Al_2O_3/YbAG ((c) Al_2O_3 and (d) YbAG)

This phenomenon has also been observed and reported in the previous work on Al_2O_3/YAG eutectic[23]. The preferred orientation of ErAG is revealed to be <111> in Fig. 4(b). For Al_2O_3/YbAG, similar to Al_2O_3/ErAG, direction <10$\bar{1}$0> was selected as the preferred growth orientation for Al_2O_3 (Fig. 4(c)), while for YbAG more than three grains with different orientations could be detected in Fig. 4(d) and no obvious preferential growth directions were established during the solidification process. We do not have an exact explanation about the phenomenon in the preferred orientation selection among Al_2O_3/REAG (RE=Y, Er, and Yb) at present. One possible reason is the surface energy discrepancy among different surfaces in REAG or the competition among different directions in REAG during the directional solidification process varied with the rare earth atoms. So, it needs a longer time or growth distance for the preferred orientation selection in YbAG phase in Al_2O_3/YbAG eutectic.

Fig. 5 depicts the pole figures of Al_2O_3/ErAG corresponding to the inverse pole figures in Fig. 4(a, b). Fig. 5(a) shows the {0001} pole figure of Al_2O_3 and Fig. 5(b) shows the {211} pole figure of ErAG, which clearly demonstrates that the orientation relationship between these two phases is {0001} Al_2O_3//{211} ErAG. According to the results in Fig. 4 and Fig. 5, the crystallographic orientation relationship in the as-prepared Al_2O_3/ErAG eutectic ceramic (at a growth distance of 80−90 mm) is as follows:

<10$\bar{1}$0> Al_2O_3//<111> ErAG;

{0001} Al_2O_3//{211} ErAG.

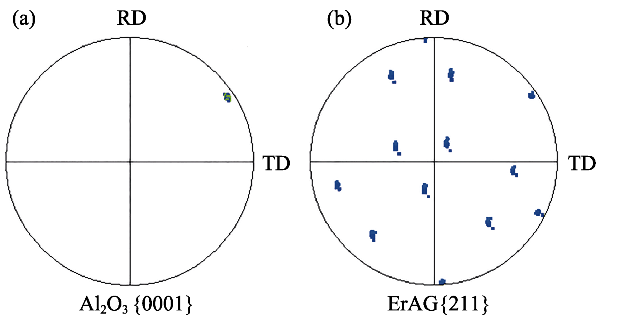

Fig. 5　Pole figures of Al_2O_3/ErAG: (a) Al_2O_3 in {0001} orientation and (b) ErAG in {211} orientation corresponding to the inverse pole figures in Fig. 4 (a) and (b)

Table 1 lists the above growth directions and orientation relationships of Al_2O_3/ErAG together with the previously reported results of some eutectic ceramics for comparison[24-28]. We can see that the growth directions of Al_2O_3 phase presented in Table 1 are quite similar although the preparation technology and eutectic system are different. The main divergence is the growth directions of REAG phase, which could be <111>, <101> and <2$\bar{1}$0>. For example, the crystallographic orientation relationship for Al_2O_3/ErAG identified by Mazerolles, *et al*. turned out to be <10$\bar{1}$0> Al_2O_3//<101> ErAG[25]. It is worth mentioning that in REAG, [111] and [101] are two directions perpendicular to each other in {211} plane and compete during the directional solidification process[29]. Similarly, both the growth directions of <111> and <101> for YAG have been detected in Al_2O_3/YAG eutectics[25-28]. We suppose that the competitive growth behavior between these two directions could be influenced by eutectic systems, solidification method, solidification parameters and so on. The detailed grain selection process and competitive growth mechanism for Al_2O_3/ErAG and Al_2O_3/YbAG eutectic ceramics will be investigated in our future work.

To characterize the distribution of Al_2O_3 and REAG phases in the directionally solidified composites more intuitively, we further reconstructed the 3D-tomographs of these two eutectics using X-ray tomography (XRT) technology. Fig. 6(a-f) illustrates the 3D-XRT images and the spatial distribution of ErAG and Al_2O_3 phases in Al_2O_3/ErAG as well as YbAG and Al_2O_3 phases in Al_2O_3/YbAG eutectic, respectively. The 3D-XRT images clearly show the continuous network of the eutectic phases in the interior of the eutectics clearly, which is commonly referred as ‘Chinese Script’ microstructure. For example, in Fig. 6(a-c), ErAG (the cobalt red phase) and Al_2O_3 (the gray phase) are interpenetrated with each other and form a geometrical 3D network. Also, utilizing the

Table 1　Growth directions and orientation relationships of some eutectic ceramics

Eutectic system	Growth method	Growth directions	Orientation relationships
Al_2O_3/ErAG	OFZ	<10$\bar{1}$0> Al_2O_3//<111> ErAG	{0001} Al_2O_3//{211} ErAG
Al_2O_3/REAG RE=Er/Yb[24]	OFZ	<10$\bar{1}$0> Al_2O_3//<101> REAG <10$\bar{1}$0> Al_2O_3//<2$\bar{1}$0> REAG	{0001} Al_2O_3//{211} REAG
Al_2O_3/YAG[25]	OFZ	<10$\bar{1}$0> Al_2O_3//<101> YAG	{0001} Al_2O_3//{211} YAG
Al_2O_3/YAG[26]	LFZ	<1$\bar{1}$00> Al_2O_3//<111> YAG	{0001} Al_2O_3//{1$\bar{1}$2} YAG
Al_2O_3/YAG[27]	Bridgman	<11$\bar{2}$0> Al_2O_3//<110> YAG <01$\bar{1}$0> Al_2O_3//<110> YAG	–
Al_2O_3/YAG[28]	LSP	<10$\bar{1}$0> Al_2O_3//<101> YAG	{0001} Al_2O_3//{211} YAG

OFZ: Optical floating zone method; LFZ: Laser floating zone method; LSP: Laser surface processing method

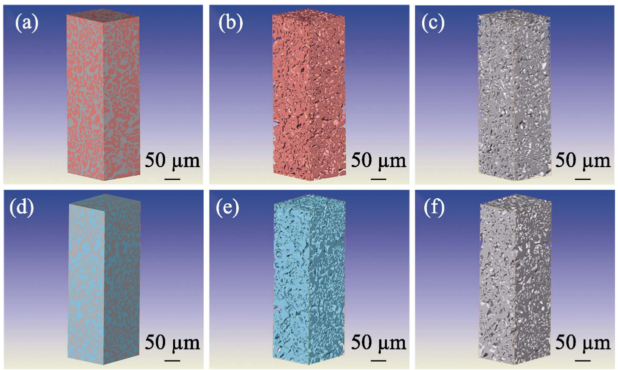

Fig. 6 3D-XRT images of directionally solidified (a) Al_2O_3/ErAG and (d) Al_2O_3/YbAG eutectics, (b, c) spatial distribution of ErAG and Al_2O_3 in Al_2O_3/ErAG, (e, f) spatial distribution of YbAG and Al_2O_3 in Al_2O_3/YbAG

3D-tomographs, we can calculate the volume fraction of the eutectic phases. For Al_2O_3/ErAG eutectic, the measured volume fraction of Al_2O_3 and ErAG are 50.5% and 49.5%, respectively, which are close to their theoretical values (Al_2O_3 51.2% and ErAG 48.8%). While for Al_2O_3/YbAG eutectic, the measured volume fraction of Al_2O_3 and YbAG are 53.5% and 46.5%, which are also consistant with the theoretical values of Al_2O_3 (55.3%) and YbAG (44.7%), respectively.

Fig. 7 presents the Vickers hardness and fracture toughness of the as prepared directionally solidified Al_2O_3/ErAG and Al_2O_3/YbAG eutectics. The Vickers hardness of Al_2O_3/ErAG and Al_2O_3/YbAG eutectics which almost remained unchanged with the variation of loads and the values tested under a load about 50 N are (13.5±0.4) and (12.8±0.1) GPa, respectively. An *E*-value of 327 GPa was taken for Al_2O_3/ErAG[15] and of 340 GPa for Al_2O_3/ YbAG[19] to calculate the fracture toughness. The fracture toughness results of Al_2O_3/ErAG and Al_2O_3/YbAG are (3.0±0.2) and (3.2±0.1) MPa·m$^{1/2}$, respectively. In Table 2, we also summarized the Vickers hardness and fracture toughness of some eutectic ceramics for comparison. Since the fracture toughness and hardness data for Al_2O_3/ErAG and Al_2O_3/YbAG prepared by optical floating zone method are not available in literatures so far, we chose the results of Al_2O_3/ErAG and Al_2O_3/YbAG prepared by laser floating zone method for comparison. Oliete, *et al.*[18-19] prepared Al_2O_3/ErAG and Al_2O_3/YbAG eutectic coatings by laser floating zone method, and the reported Vickers hardness and fracture toughness, which were tested following the same testing methods using Eq. (1) and (2), were (14.8–14.9) GPa and (1.8–2.2) MPa·m$^{1/2}$, respectively. Mesa, *et al.*[9] also prepared $Al_2O_3/Er_3Al_5O_{12}$ eutectic rods using laser-heated floating zone method with different grown speed (25–1500 mm/h). Their results indicated that the Vickers hardness increased slightly with growth rate, up to a maximum of 16 GPa, while the fracture toughness was about 1.9 MPa·m$^{1/2}$. That means that the as-prepared Al_2O_3/ErAG and Al_2O_3/YbAG eutectic ceramics exhibit slightly lower hardness and obviously enhanced fracture toughness comparing with previous works. It should be mentioned that the mechanical properties of directionally solidified eutectic ceramics, such as Vickers hardness and fracture toughness, are closely related to the preparation method and eutectic microstructure. The lamellar spacings, measured from transverse cross-section SEM micrographs for Al_2O_3/ErAG and Al_2O_3/ YbAG in Ref. [19] are (0.74±0.1) and (0.71±0.1) mm, respectively, which are much smaller than those of as-prepared Al_2O_3/ErAG and Al_2O_3/YbAG (6.9 and 17.2 μm, respectively). It is expected that this discrepancy in mechanical properties is mainly due to the difference in eutectic microstructures. Furthermore, we made some comparison with $Al_2O_3/Y_3Al_5O_{12}$ eutectic ceramic, which was prepared using the same optical floating zone method at a growth speed of 20 mm/h[24]. The Vickers hardness and fracture toughness of Al_2O_3/ YAG are 13.5 GPa and (3.1±0.3) MPa·m$^{1/2}$, respectively, which are close to the values of as-prepared Al_2O_3/ErAG and Al_2O_3/YbAG eutectics.

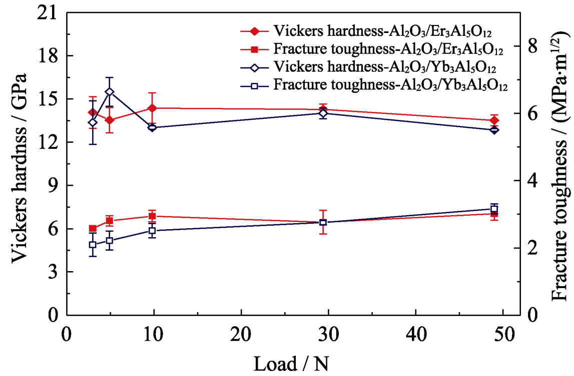

Fig. 7 Vickers hardness and fracture toughness of directionally solidified eutectics for Al_2O_3/ErAG and Al_2O_3/YbAG

Table 2 Comparison of Vickers hardness and fracture toughness of some Al_2O_3/REAG eutectic ceramics

Eutectic system	Preparation method	Vickers hardness /GPa	Fracture toughness /(MPa·m$^{1/2}$)
Al_2O_3/ErAG	OFZ	(13.5±0.4)	(3.0 ± 0.2)
Al_2O_3/YbAG	OFZ	(12.8±0.1)	(3.2 ± 0.1)
Al_2O_3/ErAG[9]	LFZ	(14.5–16.0)	1.9
Al_2O_3/ErAG[19]	LFZ	(14.9±0.7)	(1.8 ± 0.3)
Al_2O_3/YbAG[19]	LFZ	(14.8±0.6)	(2.2 ± 0.5)
Al_2O_3/YAG[24]	OFZ	13.5	(3.1±0.3)

OFZ: Optical floating zone method; LFZ: Laser floating zone method

3 Conclusions

In this work, directionally solidified Al_2O_3/ErAG and Al_2O_3/YbAG eutectic rods with uniform and homogeneous microstructures were prepared using the optical floating zone melting method. The as-grown eutectic rods are both with an average diameter in about 11 mm and length in about 90 mm, of which Al_2O_3/ErAG eutectic rod shows pink color and Al_2O_3/YbAG eutectic rod is blue. The microstructure characteristics of the as-received eutectics show that the crystallography of Al_2O_3/ErAG eutectic ceramic (at a growth distance of 80–90 mm from the seed) is: $<10\bar{1}0>$ Al_2O_3//<111> ErAG and {0001} Al_2O_3//{211} ErAG. The volume fraction of Al_2O_3 and ErAG in Al_2O_3/ErAG are 50.5% and 49.5%, respectively, while for Al_2O_3/YbAG eutectic, the volume fraction of Al_2O_3 and YbAG are 53.5% and 46.5%, respectively. The Vickers hardness of Al_2O_3/ErAG and Al_2O_3/YbAG are determined as (13.5±0.4) and (12.8±0.1) GPa, respectively. The fracture toughness results of Al_2O_3/ErAG and Al_2O_3/YbAG are (3.0±0.2) and (3.2±0.1) $MPa\cdot m^{1/2}$, respectively. The hardness values are slightly lower compared with previously reported Al_2O_3/ErAG and Al_2O_3/YbAG eutectic ceramics while the fracture toughness values show obvious enhancement comparing with previous works, which highlight the reliable mechanical properties and potential structural applications of the as-prepared Al_2O_3/ErAG and Al_2O_3/YbAG eutectic ceramics.

References:

[1] WAKU Y, NAKAGAWA N, WAKAMOTO T, *et al*. High temperature strength and thermal stability of a unidirectionally solidified Al_2O_3/YAG eutectic composite. *Journal of Materials Science*, 1998, **33:** 1217–1225.

[2] WAKU Y, NAKAGAWA N, WAKAMOTO T, *et al*. A ductile ceramic eutectic composite with high strength. *Nature*, 1997, **389:** 49–52.

[3] LLORCA J, ORERA V M. Directionally solidified eutectic oxide ceramics. *Progress in Materials Science*, 2006, **51:** 711–809.

[4] PASTOR J Y, LLORCA J, SALAZAR A, *et al*. Mechanical properties of melt-grown alumina-yttrium aluminum garnet eutectics up to 1900 K. *Journal of the American Ceramic Society*, 2005, **88:** 1488–1495.

[5] OLIETE P B, PENA J I, LARREA A, *et al*. Ultra-high-strength nanofibrillar Al_2O_3-YAG-YSZ eutectics. *Advanced Materials*, 2007, **19:** 2313–2318.

[6] ZHANG J, SU H J, SONG K, *et al*. Microstructure, growth mechanism and mechanical property of Al_2O_3-based eutectic ceramic in situ composites. *Journal of the European Ceramic Society*, 2011, **31:** 1191–1198.

[7] WAKU Y, NAKAGAWA N, OHTSUBO H, *et al*. Fracture and deformation behaviour of melt growth composites at very high temperatures. *Journal of Materials Science*, 2001, **36:** 1585–1594.

[8] MARTINEZ FERNANDEZ J, SAYIR A, FARMER S C. High temperature creep deformation of directionally solidified $Al_2O_3/Er_3Al_5O_{12}$. *Acta Materialia*, 2003, **51:** 1705–1720.

[9] MESA M C, OLIETE P B, ORERA V M, *et al*. Microstructure and mechanical properties of $Al_2O_3/Er_3Al_5O_{12}$ eutectic rods grown by the laser-heated floating zone method. *Journal of the European Ceramic Society*, 2011, **31:** 1241–1250.

[10] MESA M C, OLIETE P B, LARREA A. Microstructural stability at elevated temperatures of directionally solidified $Al_2O_3/Er_3Al_5O_{12}$ eutectic ceramics. *Journal of Crystal Growth*, 2012, **360:** 119–122.

[11] REN Q, SU H J, ZHANG J, *et al*. Microstructure control, competitive growth and precipitation rule in faceted $Al_2O_3/Er_3Al_5O_{12}$ eutectic *in situ* composite ceramics prepared by laser floating zone melting. *Journal of the European Ceramic Society*, 2019, **39:** 1900–1908.

[12] REN Q, SU H J, ZHANG J, *et al*. Halo formation in directionally solidified Al_2O_3-$Er_3Al_5O_{12}$ off-eutectic *in situ* composite ceramics. *Materials Characterization*, 2019, **150:** 31–37.

[13] REN Q, SU H J, ZHANG J, *et al*. Eutectic growth behavior with regular arrangement in the faceted $Al_2O_3/Er_3Al_5O_{12}$ irregular eutectic system at low growth rate. *Scripta Materialia*, 2019, **162:** 49–53.

[14] REN Q, SU H J, ZHANG J, *et al*. Effect of an abrupt change in pulling rate on microstructures of directionally solidified Al_2O_3-$Er_3Al_5O_{12}$ eutectic and off-eutectic composite ceramics. *Ceramics International*, 2019, **45:** 6632–6638.

[15] SAI H, YUGAMI H, NAKAMURA K, *et al*. Selective emission of $Al_2O_3/Er_3Al_5O_{12}$ eutectic composite for thermophotovoltaic generation of electricity. *Japanese Journal of Applied Physics*, 2000, **39:** 1957–1961.

[16] ADACHI Y, YUGAMI H, SHIBATA K, *et al*. Compact TPV generation system using $Al_2O_3/Er_3Al_5O_{12}$ eutectic ceramics selective emitters. *AIP Conference Proceedings*, 2004, **738:** 198–205.

[17] NAKAGAWA N, OHTSUBO H, WAKU Y, *et al*. Thermal emission properties of $Al_2O_3/Er_3Al_5O_{12}$ eutectic ceramics. *Journal of the European Ceramic Society*, 2005, **25:** 1285–1291.

[18] OLIETE P B, MESA M C, MERINO R I, *et al*. Directionally solidified Al_2O_3-$Yb_3Al_5O_{12}$ eutectics for selective emitters. *Solar Energy Materials and Solar Cells*, 2016, **144:** 405–410.

[19] OLIETE P B, MANUEL J, ROBLEDO L, *et al*. Directionally solidified Al_2O_3-$ME_3Al_5O_{12}$ (ME: Y, Er and Yb) eutectic coatings for thermophotovoltaic systems. *Ceramics International*, 2017, **43:** 16270–16275.

[20] LAKIZA S M. Directionally solidified eutectics in the Al_2O_3-ZrO_2-$Ln(Y)_2O_3$ systems. *Powder Metallurgy and Metal Ceramics*, 2009, **48:** 1–2.

[21] YOSHIKAWA A, HASEGAWA K, LEE J H, *et al*. Phase identification of $Al_2O_3/RE_3Al_5O_{12}$ and $Al_2O_3/REAlO_3$ (RE=Sm–Lu, Y) eutectics. *Journal of Crystal Growth*, 2000, **218:** 67–73.

[22] ANSTIS G R, CHANTIKUL P, LAWN B R, *et al*. A critical-evaluation of indentation techniques for measuring fracture-toughness: I, direct crack measurements. *Journal of the American Ceramic Society*, 1981, **64:** 533–538.

[23] WANG X, WANG J Y, SUN L C, *et al*. Microstructure evolution of $Al_2O_3/Y_3Al_5O_{12}$ eutectic crystal during directional solidification. *Scripta Materialia*, 2015, **108:** 31–34.

[24] MAZEROLLES L, PERRIERE L, LARTIGUE-KORINEK S, *et al*. Microstructures, crystallography of interfaces, and creep behavior of melt-growth composites. *Journal of the European Ceramic Society*, 2008, **28:** 2301–2308.

[25] WANG X, TIAN Z L, ZHANG W, *et al*. Mechanical properties of directionally solidified $Al_2O_3/Y_3Al_5O_{12}$ eutectic ceramic prepared by optical floating zone technique. *Journal of the European Ceramic Society*, 2018, **38:** 3610–3617.

[26] FRAZER C S, DICKEY E C, SAYIR A. Crystallographic texture and orientation variants in Al_2O_3-$Y_3Al_5O_{12}$ directionally solidified eutectic crystals. *Journal of Crystal Growth*, 2001, **233:** 187–195.
[27] SAKATA S, MITANI A, SHIMIZU K, *et al*. Crystallographic orientation analysis and high temperature strength of melt growth composite. *Journal of the European Ceramic Society*, 2005, **25:** 1441–1445.
[28] SU H J, ZHANG J, MA W D, *et al*. *In situ* fabrication of highly-dense Al_2O_3/YAG nanoeutectic composite ceramics by a modified laser surface processing. *Journal of the European Ceramic Society*, 2014, **34:** 739–744.
[29] WANG X, WANG D, ZHANG H, *et al*. Mechanism of eutectic growth in directional solidification of an Al_2O_3/$Y_3Al_5O_{12}$ crystal, *Scripta Materialia*, 2016, **116:** 44–48.

光悬浮区熔定向凝固 $Al_2O_3/Er_3Al_5O_{12}$ 和 $Al_2O_3/Yb_3Al_5O_{12}$ 共晶陶瓷的制备与性能研究

孙鲁超[1], 周 翠[1,2], 杜铁锋[1], 吴 贞[1], 雷一明[1,2], 李家麟[1], 苏海军[3], 王京阳[1]

(1. 中国科学院 金属研究所, 沈阳材料科学国家研究中心, 沈阳 110016; 2. 中国科学技术大学 材料科学与工程学院, 沈阳 110016; 3. 西北工业大学 凝固技术国家重点实验室, 西安 710072)

摘 要: 本研究探索了光悬浮区熔法制备 $Al_2O_3/Er_3Al_5O_{12}$(ErAG)和 $Al_2O_3/Yb_3Al_5O_{12}$(YbAG) 定向凝固共晶陶瓷。在 10 mm/h 的抽拉速率下成功获得了凝固组织均匀、内部无裂纹或孔洞的高质量共晶陶瓷。通过高分辨三维 X 射线衍射仪研究了 Al_2O_3 和 $RE_3Al_5O_{12}$ 在三维空间的分布与组织结构; 利用电子背散射衍射技术分析了定向凝固末期 Al_2O_3 和 $RE_3Al_5O_{12}$ 两相的晶体学择优取向和相界面关系。力学性能表征结果显示, Al_2O_3/ErAG 和 Al_2O_3/YbAG 具有优异的力学性能, 二者的维氏硬度分别为(13.5±0.4)和(12.8±0.1) GPa; 断裂韧性分别为(3.0±0.2)和(3.2±0.1) MPa·$m^{1/2}$。

关 键 词: 定向凝固; 共晶陶瓷; 显微结构; 力学性能

中图分类号: TQ174 **文献标志码**: A